Low-Power ECG-Based Processor for Predicting Ventricular Arrhythmia

Nourhan Bayasi, *Member, IEEE*, Temesghen Tekeste, *Member, IEEE*, Hani Saleh, *Senior Member, IEEE*, Baker Mohammad, *Senior Member, IEEE*, Ahsan Khandoker, *Senior Member, IEEE*, and Mohammed Ismail, *Fellow, IEEE*

***Abstract*— This paper presents the design of a fully integrated electrocardiogram (ECG) signal processor (ESP) for the prediction of ventricular arrhythmia using a unique set of ECG features and a naive Bayes classifier. Real-time and adaptive techniques for the detection and the delineation of the P-QRS-T waves were investigated to extract the fiducial points. Those techniques are robust to any variations in the ECG signal with high sensitivity and precision. Two databases of the heart signal recordings from the MIT PhysioNet and the American Heart Association were used as a validation set to evaluate the performance of the processor. Based on application-specified integrated circuit (ASIC) simulation results, the overall classification accuracy was found to be 86% on the out-of-sample validation data with 3-s window size. The architecture of the proposed ESP was implemented using 65-nm CMOS process. It occupied 0.112-mm^2 area and consumed 2.78-μW power at an operating frequency of 10 kHz and from an operating voltage of 1 V. It is worth mentioning that the proposed ESP is the first ASIC implementation of an ECG-based processor that is used for the prediction of ventricular arrhythmia up to 3 h before the onset.**

***Index Terms*— Adaptive techniques, application-specified integrated circuit (ASIC), classification, electrocardiography (ECG), feature extraction, low power, ventricular arrhythmia.**

I. Introduction

SUDDEN cardiac death accounts for approximately 300 000 deaths in the United States per year, and, in most cases, is the final result of ventricular arrhythmias, including ventricular tachycardia (VT) or ventricular fibrillation (VF) [1]. Ventricular arrhythmia is an abnormal ECG rhythm and is responsible for 75%–85% of sudden deaths in persons with heart problems unless treated within seconds [1]. Most ventricular arrhythmias are caused by coronary heart disease, hypertension, or cardiomyopathy, and if not accurately diagnosed nor treated, immediate death occurs [2]. VT is a fast rhythm of more than three consecutive beats originating from the ventricles at a rate more than 100 beats/min [3]. VF is another rhythm characterized by the chaotic activation of ventricles, and it causes immediate cessation of blood circulation and degenerates further into a pulseless or flat ECG signal indicating no cardiac electrical activity.

The implantable cardioverter-defibrillator has been considered as the best protection against sudden death from ventricular arrhythmias in high-risk individuals. However, most sudden deaths occur in individuals who do not have high-risk profiles. Long-term ECG monitoring is the criterion standard for the diagnosis of ventricular arrhythmia. The 12-lead ECGs are obtained and analyzed to detect any changes in the characteristics of the ECG signal. By extracting information about intervals, amplitudes, and waveform morphologies of the different P-QRS-T waves, the onset of the ventricular arrhythmia can be detected. A wide range of methods were developed to detect ventricular arrhythmia based on morphological [4], [5], spectral [6], or mathematical [7] features extracted from the ECG signal. Machine learning techniques, such as neural networks [8] and support vector machine (SVM) [9] have also been suggested as a useful tool to improve the detection efficiency. Although these methods have exhibited advantages in the detection of ventricular arrhythmia, they have some shortcomings. Some are too difficult to implement or compute, some have low specificity in discriminating between normal and abnormal conditions, and all maintain late detection interval, which is usually not enough to take an action.

A. Literature Review

Recently, due to the remarkable advancement in technology, the development of dedicated hardware for accurate ECG analysis and classification in real time has become possible. The main requirements are low-power consumption and low-energy operation in order to have longer battery lifetime along with the small area for wearability. Many attempts succeeded to implement ECG signal processing and classification systems in hardware. Shiu *et al.* [10] implemented an integrated electrocardiogram signal processor (ESP) for the identification of heart diseases using the 90-nm CMOS technology. The system employed an instrumentation amplifier and a low-pass filter (LPF) to remove the baseline wander and the power line interference form the ECG and employed

Manuscript received April 7, 2015; revised July 10, 2015; accepted August 24, 2015. Date of publication October 6, 2015; date of current version April 19, 2016. This work was supported by the Mubadala–SRC Center of Excellence for Energy Efficient Electronic Systems Research under Contract 2013-HJ2440.

N. Bayasi, T. Tekeste, H. Saleh, B. Mohammad, and M. Ismail are with the Electrical and Computer Engineering Department, Khalifa University of Science, Technology and Research (KUSTAR), and KUSTAR Semi-Conductor Research Center (KSRC), UAE (e-mail: nourhan.bayasi@kustar.ac.ae; temesghen.habte@kustar.ac.ae; hani.saleh@kustar.ac.ae; baker.mohammad@kustar.ac.ae; ismail@kustar.ac.ae).

A. Khandoker is with the Biomedical Engineering Department, Khalifa University of Science, Technology and Research, UAE (e-mail: ahsan.khandoker@kustar.ac.ae).

Color versions of one or more of the figures in this paper are available online at http://ieeexplore.ieee.org.

Digital Object Identifier 10.1109/TVLSI.2015.2475119

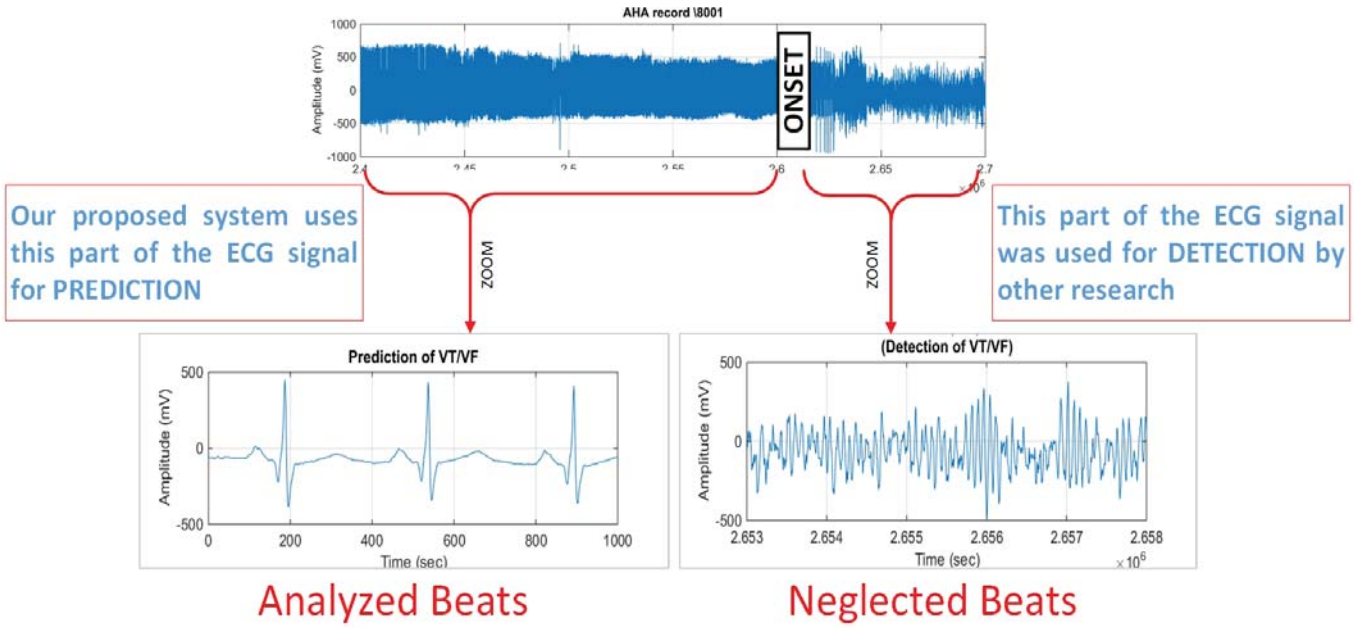

Fig. 1. Prediction versus detection of the onset of VT/VF from the ECG heartbeat analysis.

a time-domain morphological analysis for the feature extraction and classification based on the evaluation of the ST segment. The system was carried out in a field-programmable gate array and consumed a total of 40.3-μW power and achieved an accuracy of 96.6%. The main disadvantage of the system is that it uses fixed search window with predefined size to locate S and T fiducial points, which is not suitable for real-time scenarios.

Another ESP was proposed in [11]. The system was fabricated on the 0.18-μm CMOS technology and executed different functions for the three stages of preprocessing, feature extraction, and classification. The algorithm behind these functions was based on the quad level vector [12]. Moreover, the functions were all pipelined to increase hardware utilization and reduce power consumption. Besides, the system employed clock gating techniques to enable and disable each processing unit individually according to the need and it applied voltage scaling up to 0.7 V. The ECG processor consumed 6 μW at 1.8 V and 1.26 μW at 0.7 V, which is much better than the system in [10] due to the low-power techniques it employed.

One recent system for ECG classification was presented in [13] and comprised of three chips. The first chip contained the body-end circuits that were the high-pass sigma delta modulator-based biosignal processor and the ON–OFF keying transmitter. The second chip, the receiving end, had the receiver and the digital signal processing (DSP) unit. The last chip was the classifier. Discrete wavelet transform was adopted by the DSP unit for the ECG feature extraction and classification. The chip was fabricated on the 0.18-μm CMOS technology and consumed a total power of 5.967 μW at 1.2 V for the DSP unit only. The accuracy of the beat detection and the ECG classification was 99.44% and 97.25%, respectively.

On the other hand, the implanted systems have been suggested as an alternate solution to the body wearable devices and attracted much interest in the field. The main benefit of such approach is that the impact of a person's motion and his daily activities is dramatically reduced. Chen *et al.* [14] proposed a syringe-implantable ECG system for arrhythmia classification based on the state-of-the-art 65-nm CMOS process. The system acquires the ECG signal, filters it, amplifies it, and digitizes it through the analog front-end (AFE) module. The AFE contains a low-noise instrumentation amplifier, a variable gain amplifier, and a successive approximation register analog-to-digital converter. The arrhythmia detection is performed using two approaches. The first approach evaluates the variance of the RR interval and applies a simple threshold technique to distinguish between normal and abnormal intervals. In the second approach, the ECG signal is transformed into the frequency domain, and the variation in the spectrum is analyzed. The design consumed 92 nW at 0.4 V for the DSP unit. The accuracy of the classification was not stated.

B. Paper Contribution: Prediction Over Detection

This paper proposes a fully integrated low-powered ESP for the prediction of ventricular arrhythmia up to 3 h before the onset, and to the best of our knowledge, this is the first solution that performs prediction instead of detection. Previous VT-/VF-related research was mainly concerned with the detection of the VT/VF condition on and after it occurs [4]–[6], while our proposed solution performs prediction of it. In VT/VF detection, the ECG segment (or features extracted from it) that follows the onset of VT/VF is used to train the classifier in order to distinguish between normal and abnormal cases. Of course, the detection of such arrhythmia is critical, because the waveform of the ECG signal changes dramatically without following a consistent pattern, as shown in Fig. 1; however, this detection is not enough to save lives as the patient is left with a very few seconds to die. On the other hand, an early prediction of VT/VF would improve the quality

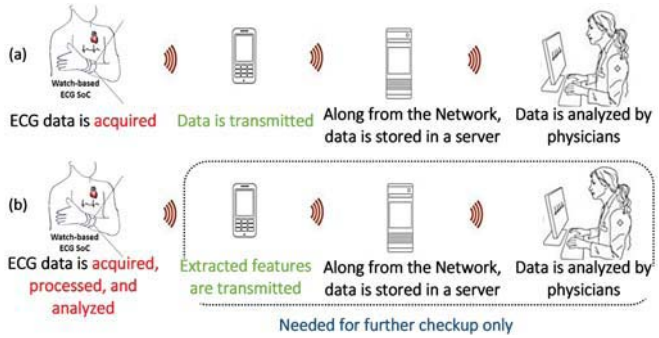

Fig. 2. Comparison between (a) commonly implemented systems and (b) proposed one.

of life by alerting the patient before any critical condition. This is achieved by analyzing the ECG segment that precedes the onset of VT/VF condition. Furthermore, the databases used for this paper enabled us to process ECG signals up to 3 h before the onset of VT/VF and attain the earliest prediction interval ever reported. The remaining part of this paper is organized as follows. In Section II, an overview of the proposed ESP is presented. Section III presents the hardware design of the ESP. The application-specified integrated circuit implementation is described in Section IV. The performance evaluation as well as a comparison against other hardware-implemented systems is reported in Section V. Finally, the conclusion is drawn in Section VI.

II. System Overview

The proposed system is a life savior for patients who are susceptible to ventricular arrhythmia by alerting them for immediate attention to their medical condition. Unlike other systems that acquire the ECG signal and transmit it for further analysis, the proposed system aims to design and develop an integrated biomedical processor that is capable of acquiring the ECG signal from the heart along with processing and analyzing it on the same chip without any external interaction, as shown in Fig. 2. Thus, the patient would have immediate alert to his situation and that is very important, especially in critical situations. Furthermore, the local processing of the data would reduce the amount of the data to be transmitted in case of any further checkup.

The proposed system consists of three main stages, which are the ECG preprocessing, feature extraction, and classification, as shown in Fig. 3. In the first stage, the ECG preprocessing is responsible for three tasks: 1) ECG filtering; 2) QRS complex detection; and 3) T and P wave delineation. The ECG filtering removes the noise coupled with the ECG signal and prepares it for further analysis. After that, the QRS complex is detected using the Pan and Tompkins (PAT) algorithm [15]. Finally, T and P waves are delineated, and the corresponding fiducial points (P onset, P peak, P offset, T onset, T peak, and T offset) are extracted. New techniques are presented in this stage to increase the robustness of the system, and this is by utilizing adaptive search windows and thresholds to accurately detect the fiducial points in each heartbeat. Each task separately is described in detail in Section III.

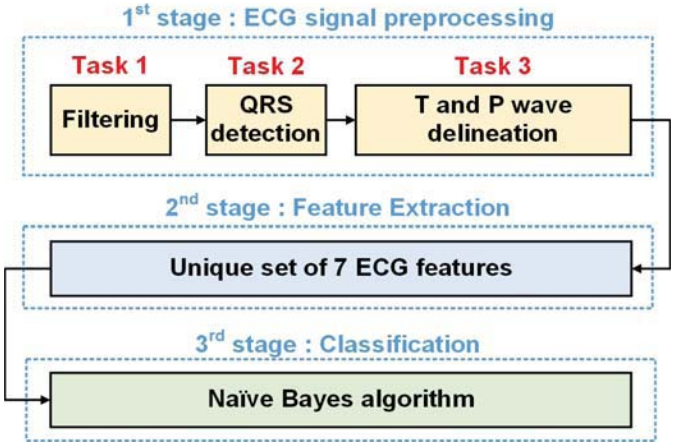

Fig. 3. Schematic representation of the proposed ventricular arrhythmia prediction system.

In the second stage, seven features are extracted from the ECG signal and grouped together to construct a unique set. All the features represent different intervals from the ECG signal, and they are RR, PQ, QP, RT, TR, PS, and SP intervals. Usually, the reported systems in the literature build their systems depending on one feature only, such as the heart rate interval [4], the variability of the timing delay of the ECG segments [5], or the QT interval variability [16]. However, multiple features were necessary to enhance the robustness of the system, and thus, we constructed this unique set of ECG intervals and used it as input for the final stage. The combination of these features has never been used in any published detection or prediction method, yet it was proved to be the most significant combination.

In the final stage, naive Bayes algorithm is used to identify the signals that are susceptible to ventricular arrhythmia. There are many reasons for choosing the naive Bayes. First, the ECG features have shown strong potential in the prediction of ventricular arrhythmia with a p-value < 0.001. Second, it was intended to investigate the performance of the system without introducing the strong biasing effect of a classifier. Finally, naive Bayes is the simplest classification method that can be easily implemented in hardware.

III. Hardware Design

The architecture of the proposed ESP is shown in Fig. 4. The architecture includes the modules of the three stages along with a main FSM that controls the flow of the data between the different stages, as shown in Fig. 5. The processing of the data is done using fixed point representation. The digitized ECG data are applied in series (from testbench) at the input to the preprocessing stage with a resolution of 8 bit, while a variable number of bits were utilized in the different stages to enhance the accuracy and avoid truncations errors.

A. ECG Preprocessing Stage

1) ECG Filtering: The block diagram of the preprocessing stage is shown in Fig. 6. Bandpass filtering of the raw ECG signal is the first step in which the filter isolates the

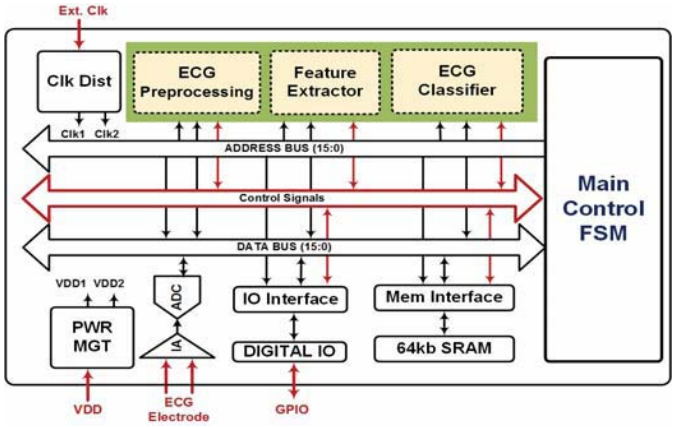

Fig. 4. Architecture of the proposed ESP.

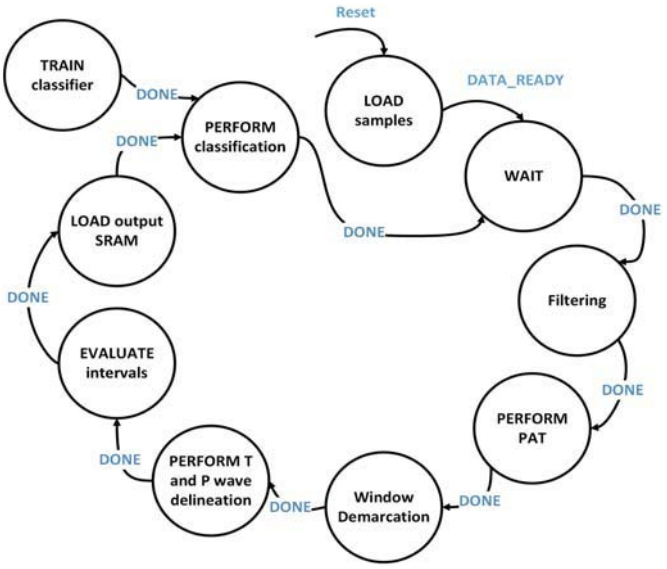

Fig. 5. Main control FSM.

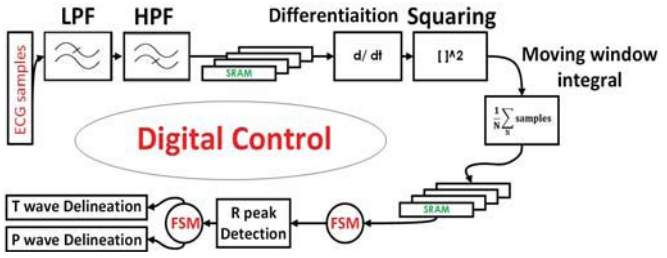

Fig. 6. Block diagram of preprocessing stage, which contains filtering, QRS detection, and P and T wave delineation.

predominant QRS energy centered at 10 Hz, and attenuates the low frequencies characteristic of the P and T waves, baseline drift, and higher frequencies associated with electromyographic noise and power line interference. The main important point is not to loose the information carried by the ECG signal after being filtered out.

The difference equations of the cascaded LPF and high-pass filter (HPF) are given in (1) and (2), respectively. The cutoff frequency of the LPF filter is 11 Hz, and it introduces a delay of six samples, whereas the HPF has a cutoff frequency and delay of 5 Hz and 16 samples, respectively. The coefficients of the filters are all integers and of power-of-two, which make them suitable for hardware implementation

$$y(nT) = 2y(nT-T) - y(nT-2T) + x(nT) - 2x(nT-6T) + x(nT-12T) \quad (1)$$

$$y[nT] = x(nT-16T) - \frac{1}{32}[y(nT-T) + x(nT) - x(nT-32T)]. \quad (2)$$

2) QRS Detection: To detect the QRS complex, the PAT method was used [15]. The PAT is a widely used method, which is based on the amplitude threshold technique exploiting the fact that R peaks have higher amplitudes compared with other ECG wave peaks [15]. With proper filtering of the signal, the method is highly capable of detecting the R peaks in every heartbeat using two threshold levels.

After filtering, the PAT algorithm is decomposed into four steps. Differentiation of the filtered signal is used to distinguish the QRS complex from other ECG waves by finding high slopes. Then, a nonlinear transformation is performed through point-to-point squaring of the filtered ECG signal in which it is important to emphasize the higher frequencies in the signal obtained from the previous step, which are normally characteristic of QRS complex. After that, integration is carried out by a moving time window to extract additional features, such as the QRS width. Finally, adaptive amplitude thresholds are applied to the averaged signal to detect R peaks. Both the bandpass filtered signal and the averaged signal are stored in separate SRAMs for further analysis.

For real-time hardware implementation, we have modified the peak detection technique, as shown in Fig. 7. Initially, the design reads the first 200 ECG samples from the SRAM, which stores the samples of the averaged ECG signal. The maximum value among these samples is set as an initial R peak and used to compute the initial value of the threshold, Th, which is set to 50% of the peak value. Then, the value of every incoming sample is compared with Th, and only the sample value, which is greater than the threshold, is used in the next step. If none of the samples have a higher value than Th, the algorithm redefined the value of the threshold and set it to 30% of the peak value ($\mathrm{Th_{sb}}$). As soon as the demarcation of the samples that exist in the QRS complex region is done, the maximum value among them is set as a new R peak, and the threshold is updated accordingly (50% of the last detected R peak). The process repeats itself, and the threshold is adjusted according to the last detected R peak. The last step in the QRS complex detection is to find the corresponding R peaks in filtered signal, which is done by subtracting the delay encountered due to the filters.

3) T and P Wave Delineation: The delineation of T and P waves is based on a novel technique proposed in [17]. The method is based on adaptive search windows along with adaptive thresholds to accurately distinguish T and P peaks from noise peak. In each heartbeat, the QRS complex is used as a reference for the detection of T and P waves in which two regions are demarcated with respect to R peaks. These regions are then used to form the forward and backward search windows of the T and P waves, respectively, as shown

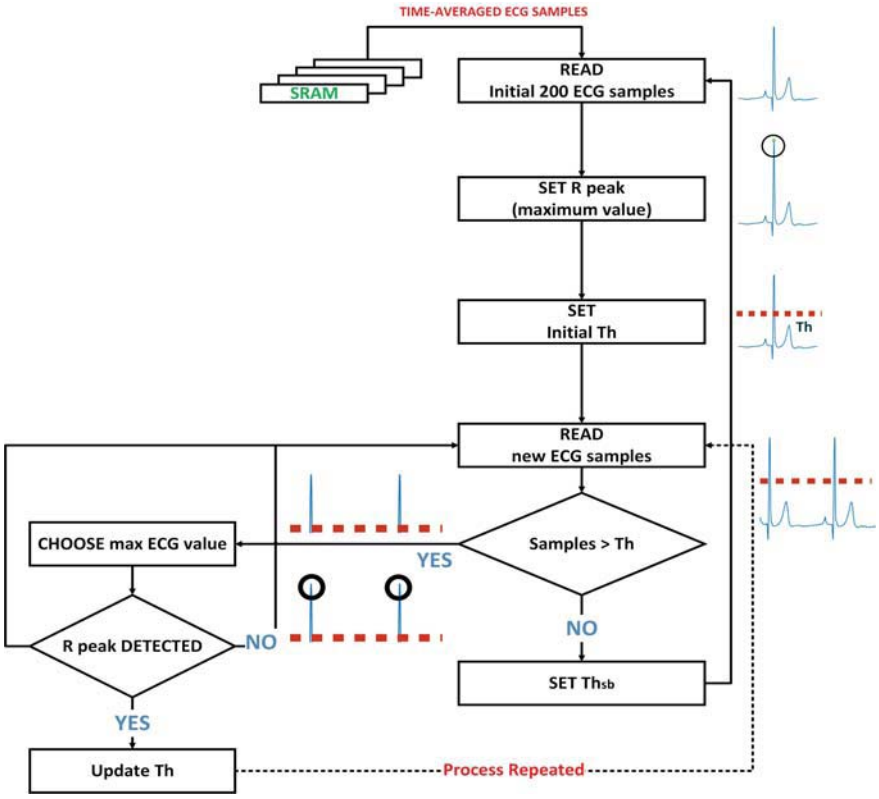

Fig. 7. Flowchart of PAT peak detection technique.

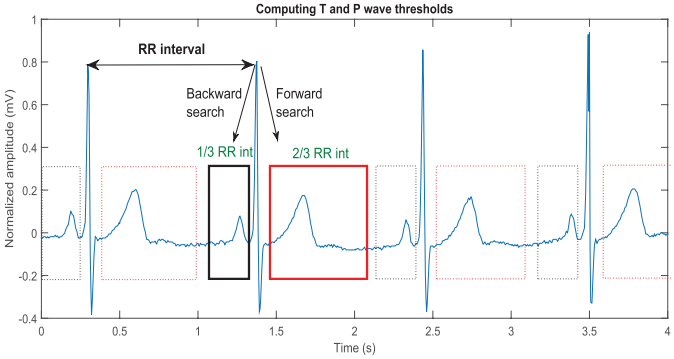

Fig. 8. Formulation of T and P wave search windows with respect to the previously calculated RR interval.

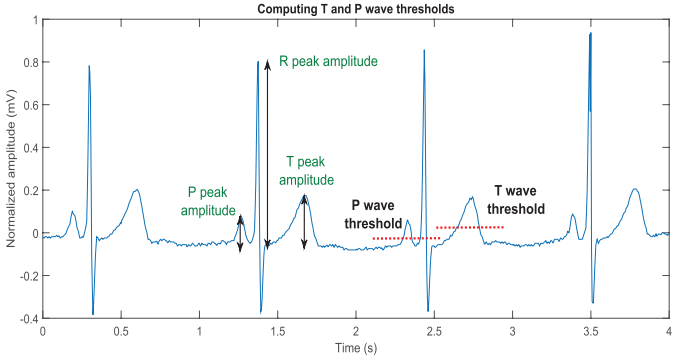

Fig. 9. Computing T and P wave thresholds based on the previously detected T peak, P peak, and R peak values.

in Fig. 8. A forward search window is assumed to contain the T wave, and the boundaries are extended from the QRS offset to two third of the previously detected RR interval. Similarly, a backward search window for the P wave is identified and extended from the QRS onset backwardly to one third of the previous RR interval.

The position of T and P peaks is demarcated in their respective search windows by finding the local maximum or/and local minimum that are above the associated thresholds. The thresholds, given in (3) and (4), are modified in each heartbeat based on the most recent detected values in the last 3 s

$$\mathrm{T}_{\mathrm{wave_{th}}} = \frac{\mathrm{T}_{\mathrm{peak}}}{\mathrm{R}_{\mathrm{peak}}} t_{\mathrm{thresh_{in}}} \tag{3}$$

$$\mathrm{P}_{\mathrm{wave_{th}}} = \frac{\mathrm{P}_{\mathrm{peak}}}{\mathrm{R}_{\mathrm{peak}}} p_{\mathrm{thresh_{in}}}. \tag{4}$$

From (3) and (4), $t_{\mathrm{thresh_{in}}}$ and $p_{\mathrm{thresh_{in}}}$ are set between 0.1 and 0.2 based on the most recent detected values in the last processing window. The technique of computing the thresholds is shown in Figs. 9 and 10. By comparing the local maximum or/and the local minimum points with the thresholds, the waveform morphology of each wave is identified [positive monophasic, inverted, or biphasic $(+,-)/(-,+)$]. If the value of T or P peak is greater than the associated threshold, then the T or P wave has a positive monophasic waveform, and the local maximum is stored to give a probable position of the peak. Otherwise, the waveform is identified as inverted, and the local minimum of the ECG signal within the same window is the correct peak. In case of biphasic wave, both the local maximum and the absolute value of the local minimum should be greater than the threshold.

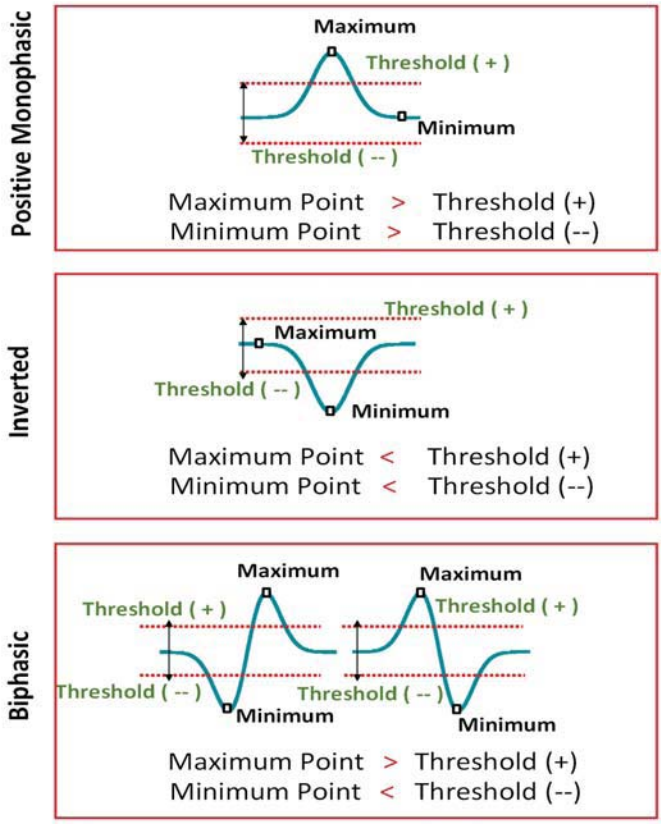

Fig. 10. T and P peaks detection. Comparing the local maximum and minimum points in each designated wave with the threshold.

4) Onset and Offset Point Delineation: The method traces the onset and offset values of the P-QRS-T waves by finding the sample corresponding to the zero slope of the entitled ECG signal. The sample point that has a zero slope and former to the peak is identified as the onset point. Similarly, the offset point is determined at other side of the peak. Sometimes, however, a derivative sign change occurs, which reflects a false indicator. To solve this, the method adds another criterion for a correct delineation of the wave boundaries based on the fact that the fiducial points tend to merge smoothly with the isoelectric line. The isoelectric line is approximated as the average value of the beat signal after removing the QRS complex. This idea is utilized and combined with the zero slope for an accurate and reliable delineation of the fiducial points. The general FSM, which illustrates the delineation process of T and P waves, is shown in Fig. 11.

B. Feature Extraction Stage

The two main parameters that must be considered while developing a detection (or prediction) system are the complexity and the accuracy of the feature extraction technique in providing the best results. For example, if the technique that is used for the feature extraction requires complex transformation or data analysis of the ECG signal, this would increase the overall cost and complexity of the system, and thus, it will not be suitable for wearable biomedical devices. For example, a technique reported in [18] is based on ECG morphology and RR intervals, leading to a simple and easily realizable

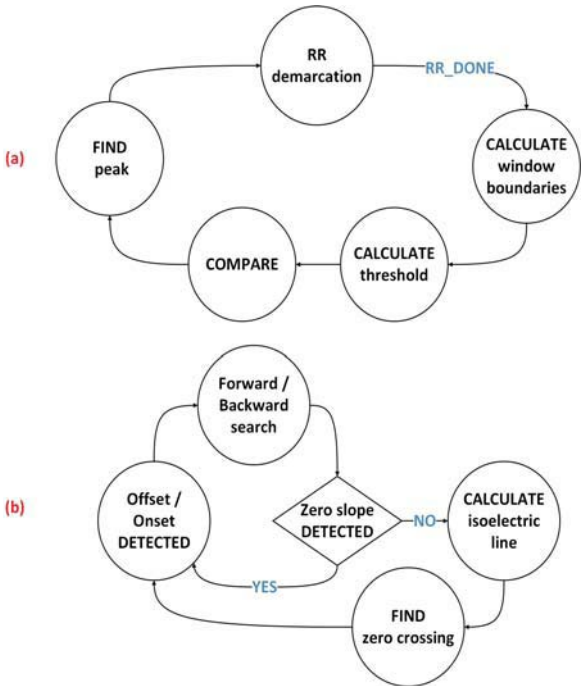

Fig. 11. FSM of T and P wave delineation. (a) Peak detection. (b) Onset and offset delineation.

detection system. On the other hand, Jen and Hwang [19] and Zhao and Zhang [20] used neural networks and a combination of wavelet transform and SVM to extract the features from the ECG signal, respectively. These techniques are more complex-to-realize and resulted in higher cost of the system. Furthermore, the extracted ECG features should show a significant relevance in the detection (or prediction) of the targeted arrhythmia to guarantee maintaining a high accuracy. Usually, there is a tradeoff between the complexity and the accuracy. For instance, the accuracy of the system in [18] is lower compared with the one presented in [19] and [20].

In this paper, both the complexity and the accuracy are addressed at the same time. To do so, we have performed statistical analysis techniques that are famous in the decision making in the biomedical research to choose the best discriminative ECG features that would maintain low system complexity and high accuracy. These statistics assist the researchers to conclude about the significance of a conducted research, and it included the mean error and standard deviation, the two-sided unpaired t-test [21], and the area under the receiver operator characteristic curve [22].

The result of such analysis yielded in a unique set of ECG features, which were found to be the most indicative characteristics of ventricular arrhythmia with a simple-to-realize system and high prediction accuracy. The features include RR, PQ, QP, RT, TR, PS, and SP intervals. Fig. 12 shows these intervals on ECG record. It is worth mentioning that the features are extracted from two consecutive heartbeats, unlike other methods that process each heartbeat independently.

C. Classification Stage

The choice of classifier in this paper was the naive Bayes. The naive Bayes classifier is easy to build with no complicated

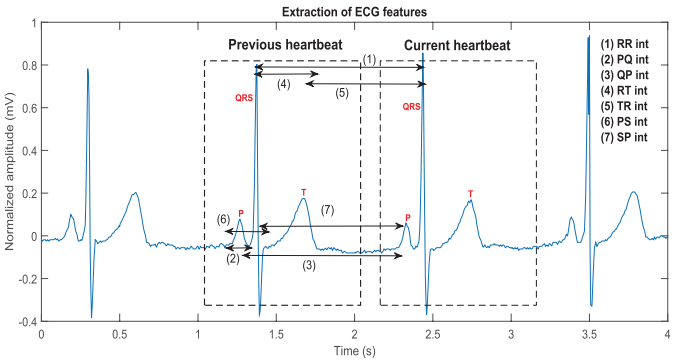

Fig. 12. ECG feature extraction from two consecutive heartbeats.

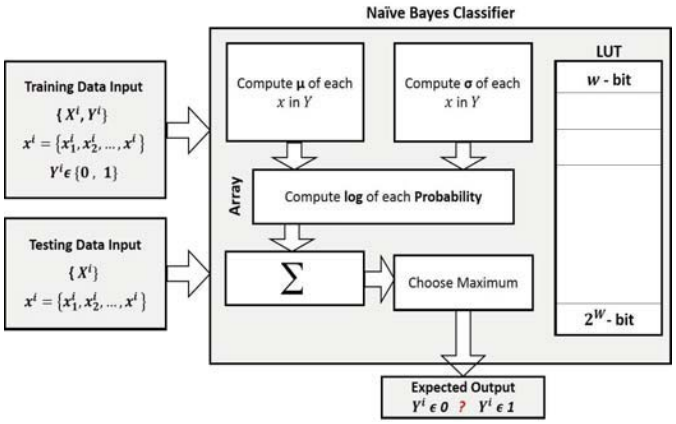

Fig. 13. Architecture of naive Bayes classifier.

iterative parameter estimation, which makes it particularly useful for hardware implementation. It assumes naive and strong independent distributions between the feature vectors, and this assumption was met, since all the extracted ECG features were independently analyzed and assessed from the beginning. The architecture of the classifier is implemented, as shown in Fig. 13.

The Bayesian classifier uses Bayes theorem to find out the probability of a data belonging to a particular class given observations. For a set of feature vectors d and class c_i, the Bayes theorem is given in

$$P(c_i \mid d) = \frac{P(d \mid c_i)P(c_i)}{P(d)}. \tag{5}$$

The best class to assign data is the one that maximizes this conditional probability out of all the classes. This can be represented by the following:

$$c = \text{argmax } P(c_i \mid d) \tag{6}$$

$$c = \text{argmax } P(c_i) \prod_x P(x \mid c_i). \tag{7}$$

And thus

$$c = \text{argmax } P(c_i) \prod_x P(x \mid c_i). \tag{8}$$

Due to the fact that calculating the product of the above probabilities will lead to float point underflow, the product operation is converted into summation by using log. Thus, instead of choosing the class with the highest probability, we choose the one with the highest log score. Given that the logarithm function is monotonic, the decision remains the same. Therefore, (9) can be calculated as follows:

$$c = \text{argmax } \left[\log(P(c_i)) + \sum_x \log(P(x \mid c_i)) \right]. \tag{9}$$

The values of each feature vector associated with each class are distributed according to Gaussian. Hence, the likelihood conditional probability of a given value v from a feature vector x given a class c_i, $P(v \mid c_i)$, is evaluated using (10), where μ and σ^2 are the mean and the variance of the values of x associated with class c_i and are given in

$$P(x = v \mid c_i) = \frac{1}{\sigma\sqrt{2\pi}} e^{-(v-\mu)^2/2\sigma^2} \tag{10}$$

$$\mu = \sum_{i=1}^{N} (x_i) \tag{11}$$

$$\sigma^2 = \frac{1}{N} \sum_{i=1}^{N} (x_i - \mu)^2. \tag{12}$$

The log of the probabilities is calculated using a lookup table (LUT) whose entries are w-bit wide and 2^w-bit deep ($w = 8$ bit). The entries in the LUT are represented in two's complement format. For any unclassified new value, we build the Gaussian model by computing the above equations from the training data set for each class. In our case, we have two classes only, GROUP A and GROUP B, which simplifies the process even more. The training data are stored in an off-chip memory because of its size. The pseudocode of both the training and testing algorithms is presented in Algorithms 1 and 2, respectively.

Algorithm 1 Training Gaussian Naive Bayes Classifier

```
procedure TRAINNAIVEBAYES
    X ← Extract Feature
    N ← Count Values
    for each c ∈ Class
    do N_c ← Count Values in c
    prior [c] ← N_c / N
    do μ ← Σ_{i=1}^{N_c} (X_i)
    do σ^2 ← (1/N_c) Σ_{i=1}^{N_c} (X_i − μ)^2
    for each V ∈ X
    do condprob [v][c] ← LUT
    return prior, condprob
```

IV. ASIC Implementation

A. Placement and Route

The ESP was designed using Verilog-HDL and implemented using an automatic synthesize, place, and route approach. A low-power industry standard 65-nm process was used for the implementation with standard cell library carefully designed

Algorithm 2 Testing Gaussian Naive Bayes Classifier

```
procedure TESTNAIVEBAYES (PRIOR, CONDPROB)
    Z ← Extract Feature
    for each c ∈ Class
    do c = condprob [c][Z]  ← LUT
    return argmax c
```

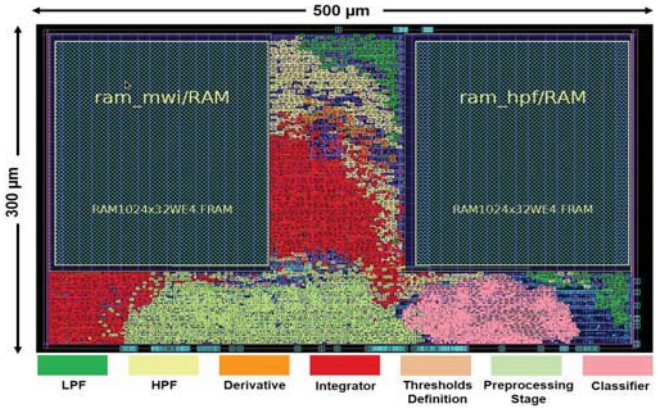

Fig. 14. Floorplan of the proposed ESP.

TABLE I
ESP IMPLEMENTATION DATA

Parameter	Figure
Combinational area	0.018 mm^2
Total cell area	0.112 mm^2
Internal power	$3e^{-4}$ mW
Switching power	$1.22e^{-5}$ mW
Leakage power	2.46 μW
Total power	2.78 μW
Utilization	85%

for low-power applications. The routing was limited to metal layer-5. Fig. 14 shows the floorplan of the design with a key to the major building blocks. The size of the ESP was defined as 500 μm $\times$ 300 μm with a total utilization of 85%. Table I presents the implementation data of the design. The design occupied a total core area of 0.112 mm^2 and consumed a total statistical power of 2.78 μW at 10-kHz frequency.

The overall architecture is designed to make it suitable for a low-power application. All the stages are pipelined by adding a significant enhancement in the throughput, and each stage is active only when a new sample is available for processing. This reduces the overall switching power. Since the preprocessed samples (output of the filtering) are available in memory, it gives the system the capability to dynamically scale the operating frequency independent of the sampling frequency. The power consumption was estimated using synthesis tools from Synopsys. Further enhancements in power dissipation could be obtained by lowering the supply voltage and using multiple voltage designs. Even though we have only reported a single supply system, the system could be expended for a multiple voltage design.

B. Timing

The placed, routed, and tapeout ready ECG processor met the timing for setup and hold at that a target frequency of 10 kHz using industry standard STA tools, and an extracted and back-annotated netlist was analyzed. Fig. 15 shows the critical timing path of the design. The design was implemented and evaluated using a standard logic library characterized at typical process, a supply voltage of 1 V and at an operating temperature of 25 °C. The critical path, as shown in Fig. 15, arises from the architectural design and from the placement of the various components in the design. Some blocks, such as the main control FSM, require multiple connections from the various modules. The PNR tool always picks the optimized location by looking the overall design.

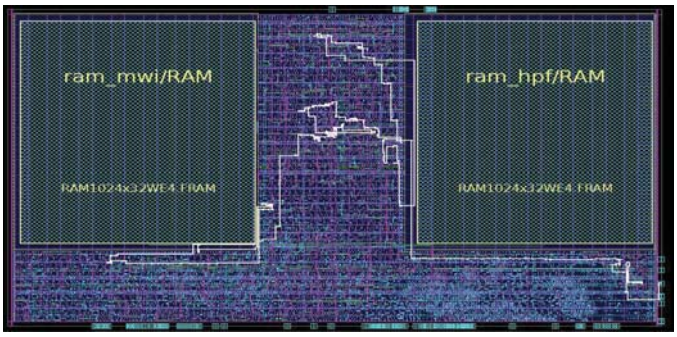

Fig. 15. Critical timing path of the design.

V. PERFORMANCE AND RESULTS

Apart from MATLAB simulations, extensive Verilog simulations were done using Modelsim and Synopsys tools to verify the working of the design. In general, the end-to-end system was implemented in Verilog-HDL, and a testbench was created to simulate it by modeling the input data. The input signal is a digitized ECG data sampled at 250 Hz. Furthermore, the system is verified to operate for different clock frequencies, and we have reported the performance for operating frequency ranging from 10 kHz up to 4 MHz. Modelsim is used as simulation and verification tool, while Synopsys digital design tools are used for synthesizing, placing, routing, and estimating area and power consumption.

A. ECG Databases

ECG recordings from the PhysioNet [23] and the American Heart Association (AHA) [24] databases were used to construct the study data sets of this paper. This paper included two groups; GROUP A included a set of five single-lead normal ECG records obtained from the NSRDB [23] and sampled at 250 Hz. These records have no significant arrhythmias. Group B involved a total of six single-lead beat-by-beat annotated abnormal ECG records with significant ventricular arrhythmias. These records have shown serious abnormality and were obtained from two sources, including the AHA [24] (records sampled at 250 Hz) and the MIT-BIH [23] (records sampled at 360 Hz). All the selected ECG records were annotated with `N` (normal heartbeat) and `[` and `]` (start/ end of VF, VT, or flutter). Furthermore, our analysis used a window of 3 s on the time before the onset of ventricular arrhythmia. The analysis was performed by moving the window from

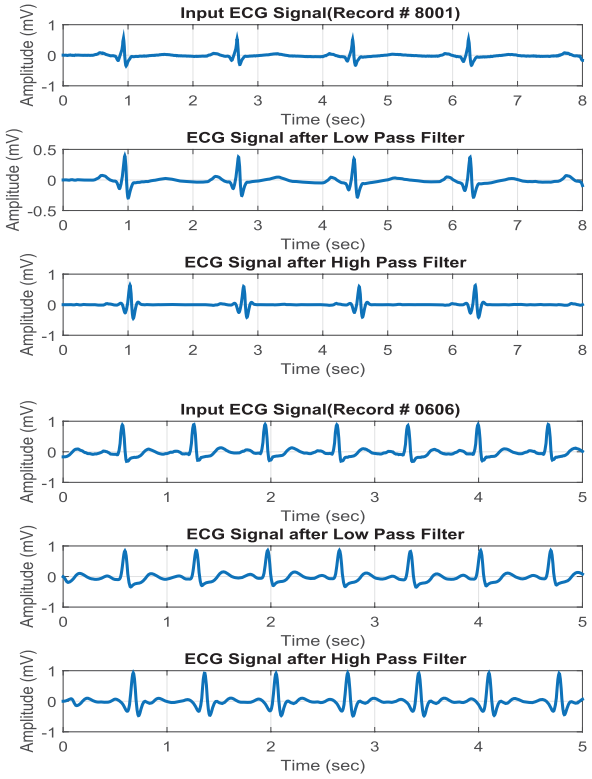

Fig. 16. Verilog results of the filtering process for different ECG records.

a few seconds before the onset, where the signal behaves quite properly, up to the associated length of each record. With such analysis, it was possible to predict the VT/VF onset even before 3 h, which is the earliest prediction duration reported so far.

B. Results of the ECG Preprocessing Stage

The filtering of the ECG signal was done through a cascaded LPF and HPF. The two filters have shown a good performance in cleaning up the ECG signal from the coupled noise, as shown in Fig. 16, where it represents the output of the filters for multiple scenarios of ECG records obtained from the PhysioNet [23] and the AHA [24] databases.

Moreover, the performance of the implemented QRS complex detector was calculated between the annotated and automated results. It was assessed by evaluating the sensitivity (SE) and precision (P) as shown in

$$\text{SE} = \frac{\text{TP}}{\text{TP} + \text{FN}} \tag{13}$$

$$P = \frac{\text{TP}}{\text{TP} + \text{FP}} \tag{14}$$

where TP stands for the number of true detections, FN denotes the number of false negative detections, and FP refers to the number of false positive detections. The QRS complex detector achieved a sensitivity of SE $= 99.83\%$ and a precision of $P = 98.65\%$.

Moreover, the mean error (μ) and the standard deviation (σ) of the fiducial points, including P peak, P offset, Q onset, R peak, S offset, T peak, and T offset, were calculated with

TABLE II
PERFORMANCE EVALUATION OF THE ECG SIGNAL PROCESSING TECHNIQUE: VERILOG RESULTS

Parameter	P_{peak}	P_{off}	Q_{on}	R_{peak}	S_{off}	T_{peak}	T_{off}
μ (ms)	10.3	9.89	8.1	6.5	1.1	3.6	-9.6
σ (ms)	15.3	14.2	11.2	8.41	9.41	12.1	20.1

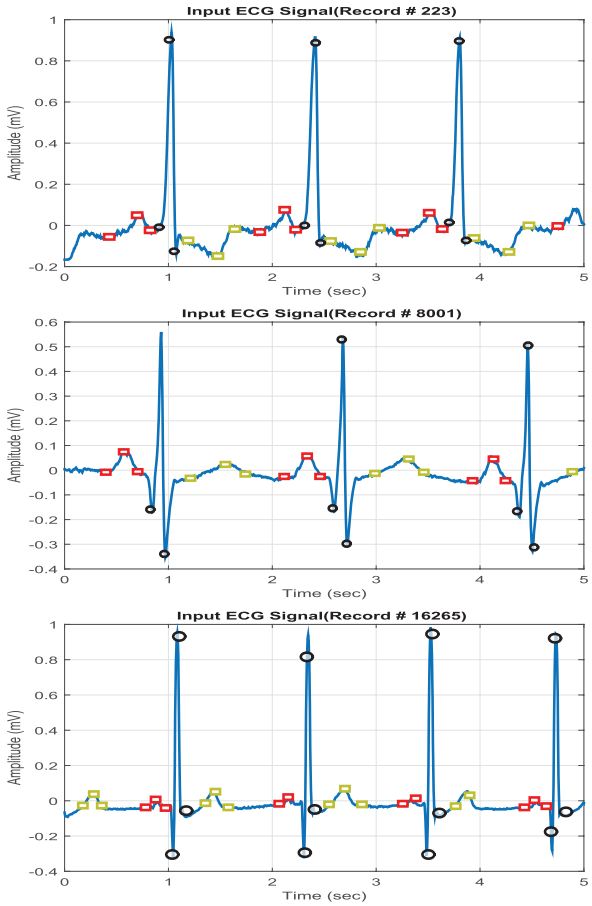

Fig. 17. Verilog results of QRS detection and T and P wave delineation for different ECG records.

a reference to the annotations, and the results are displayed in Table II. The performance of the technique is highly accurate and satisfactory for advanced ECG feature extraction. Fig. 17 highlights the capability of the system to detect and delineate the ECG signal in different real-life scenarios. We have tried four real-time ECG records obtained from the PhysioNet and the AHA databases and tested the system on them. It is clear from Fig. 17 that the system works with different variations of ECG waveform morphologies and can identify all the waves of the ECG signal. Of course, identifying the different ECG waves is much needed and a crucial step to do further analysis and be able to correctly extract more information from the signal.

C. Results of Classification Stage

The classification results, which were obtained after simulating the ECG data in Modelsim, are presented in Table III.

TABLE III
PERFORMANCE EVALUATION OF THE ECG SIGNAL PROCESSING TECHNIQUE: VERILOG RESULTS

Overall Result	Percentage (%)
True Positive (TP)	84.26
True Negative (TN)	87
False Negative (FN)	15.74
False Positive (FP)	13

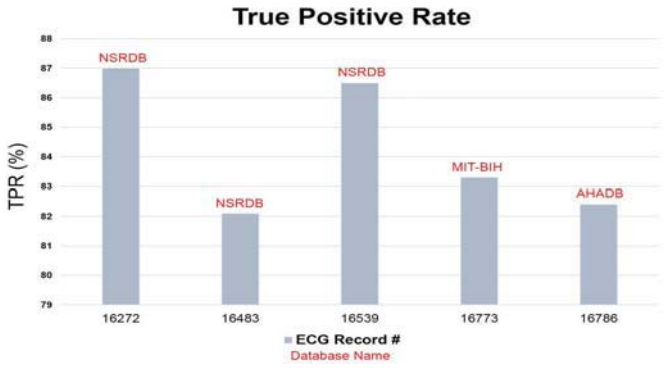

Fig. 18. Percentage of TPR in GROUP A records.

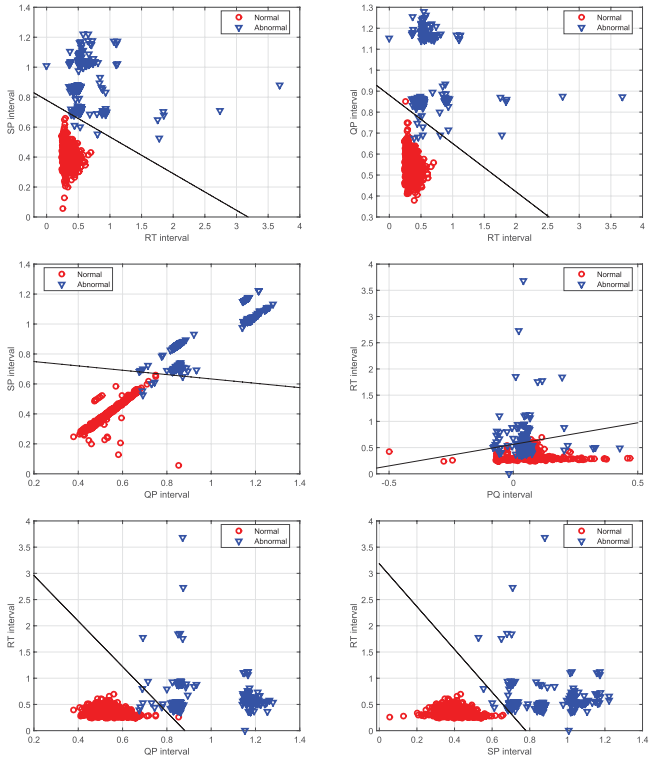

Fig. 19. Geometric representation of the distribution of some pair of intervals for two classes.

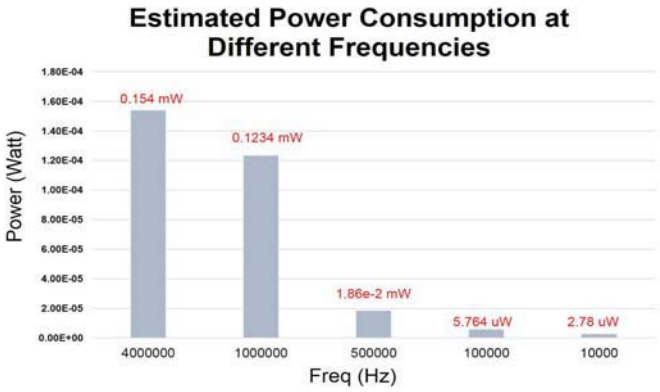

Fig. 20. Tradeoff between the operating frequency and the consumed power.

These results are based on the classifier output on 3-s processing window. The classification accuracy is computed as in (15) and found to be 86% (TN refers to the number of true negative detections). Moreover, the TP rate (TPR) of GROUP A records is shown in Fig. 18 with the TPR of 87% and 82.1% as the best and worst cases, respectively

$$\text{ACC} = \frac{\text{TP} + \text{TN}}{\text{TP} + \text{TN} + \text{FP} + \text{FN}}. \tag{15}$$

A geometric representation of the classification output for some pair of feature vectors that are associated with two classes is shown in Fig. 19. The two classes are represented in red circles for normal ECG signals and blue triangles for ECG signals with VT/VF rhythms.

D. Comparison Against Others

The performance of the proposed ESP was compared against four other published designs from the literature, and the comparison details are shown in Table IV. This paper is using the smallest technology, 65 nm, and thus, it resulted in the smallest possible area among the others, 0.112 mm^2 with an operating frequency of 10 kHz and from a voltage supply of 1 V. It is worthy knowing that the reported power in Table IV varies among the other presented work due to the fact that different frequencies and voltage supplies along with different technologies were used. To show the effect of scaling the frequency on our system, we run the design at different clock frequencies ranging from 10 kHz to 4 MHz at a supply voltage of 1 V, and Fig. 20 shows the estimated power consumed at those frequencies. All essential features of the ECG signal are concentrated at low frequencies (less than 150 Hz), and the ECG is sampled at <1 kHz. Hence, an operating frequency of 10 kHz is more than sufficient to adequately process an ECG signal. At this frequency, our system consumed only of 2.78 μW that deems it very suitable for wearable devices. Moreover, the architecture of the system was designed suitable for ultralow power consumption. A substantial amount of work was done in optimizing the RTL code in order to lower the power consumption. Switching power was reduced by implementing some components of the system using combinational circuits.

Furthermore, the proposed system is the only one that is used for the prediction of ventricular arrhythmia (refer to Table IV), while all the rest do detection of it. This is the most important contribution in this paper, which

TABLE IV
COMPARISON OF ESP HARDWARE IMPLEMENTED DESIGNS

Reference	Technology (μm)	Area (mm^2)	Power (μW)	Supply Voltage (V)	Frequency (KHz)	Detection Accuracy (%)	Prediction Accuracy (%)	Type
[11]	0.18	2.25	1.26	0.7	1	NA	NA	SoC
[13]	0.18	2.4649	5.967	1.2	0.12	97.25	NA	SoC
[14]	0.065	3.3205	0.095	0.4	10	NA	NA	SoC
This work	**0.065**	**0.112**	**2.78**	**1.0**	**10**	**NA**	86	**ASIC**

believed to be a life savior to many patients with ventricular arrhythmias.

VI. CONCLUSION

In this paper, a fully integrated digital ESP for the prediction of ventricular arrhythmia that combines a unique set of ECG features with naive Bayes was proposed. Real-time and adaptive techniques for the detection and delineation of the P-QRS-T waves were investigated and employed to extract the fiducial points. Furthermore, seven features that represent different intervals of the ECG signal were extracted and used as input to the naive Bayes to classify each heartbeat as normal or abnormal. The combination of these features has never been used in any previous detection or prediction system. The ESP was implemented using the state-of-the-art 65-nm technology, and based on the design constraints, it occupied an area of 0.112 mm^2 and consumed a total power of 2.78 μW. Moreover, the proposed ESP achieved an outstanding capability of predicting the arrhythmia up to 3 h before the onset. A prediction accuracy of 86% was obtained on the out-of-sample validation data by tenfold cross validation with 3-s window size. The small area, low power, and high performance of the proposed ESP make it suitable for inclusion in system on chips targeting wearable mobile medical devices.

The improvements that will be added to this design in the future could be summarized as follows.

1) Integrate multiple biomedical signals with the ECG, such as blood glucose, electroencephalograph, and electromyography.
2) Include a low-powered wireless transceiver module to transmit the biomedical signals.
3) Employ different filtering techniques to remove any type of noise that could be coupled with the ECG signal.
4) Employ a search-back mechanism in case of miss detection of any of the P-QRS-T waves.
5) Employ some power reduction techniques, such as clock and frequency scaling.

REFERENCES

[1] J. W. Schleifer and K. Srivathsan, "Ventricular arrhythmias: State of the art," *Cardiol. Clin.*, vol. 31, no. 4, pp. 595–605, 2013.

[2] D. P. Zipes and H. J. J. Wellens, "Sudden cardiac death," *Circulation*, vol. 98, no. 21, pp. 2334–2351, 1998.

[3] C. J. Garratt, *Mechanisms and Management of Cardiac Arrhythmias*. London, U.K.: BMJ Books, 2001.

[4] P. de Chazal, M. O'Dwyer, and R. B. Reilly, "Automatic classification of heartbeats using ECG morphology and heartbeat interval features," *IEEE Trans. Biomed. Eng.*, vol. 51, no. 7, pp. 1196–1206, Jul. 2004.

[5] A. Amann, R. Tratnig, and K. Unterkofler, "Detecting ventricular fibrillation by time-delay methods," *IEEE Trans. Biomed. Eng.*, vol. 54, no. 1, pp. 174–177, Jan. 2007.

[6] O. Sayadi, M. B. Shamsollahi, and G. D. Clifford, "Robust detection of premature ventricular contractions using a wave-based Bayesian framework," *IEEE Trans. Biomed. Eng.*, vol. 57, no. 2, pp. 353–362, Feb. 2010.

[7] X.-S. Zhang, Y.-S. Zhu, N. V. Thakor, and Z.-Z. Wang, "Detecting ventricular tachycardia and fibrillation by complexity measure," *IEEE Trans. Biomed. Eng.*, vol. 46, no. 5, pp. 548–555, May 1999.

[8] J. Pardey, "Detection of ventricular fibrillation by sequential hypothesis testing of binary sequences," in *Proc. IEEE Comput. Cardiol.*, Sep./Oct. 2007, pp. 573–576.

[9] Q. Li, C. Rajagopalan, and G. D. Clifford, "Ventricular fibrillation and tachycardia classification using a machine learning approach," vol. 61, no. 3, pp. 1607–1613, Jun. 2013.

[10] B.-Y. Shiu, S.-W. Wang, Y.-S. Chu, and T.-H. Tsai, "Low-power low-noise ECG acquisition system with dsp for heart disease identification," in *Proc. IEEE Biomed. Circuits Syst. Conf. (BioCAS)*, Oct./Nov. 2013, pp. 21–24.

[11] H. Kim, R. F. Yazicioglu, T. Torfs, P. Merken, H.-J. Yoo, and C. Van Hoof, "A low power ECG signal processor for ambulatory arrhythmia monitoring system," in *Proc. IEEE Symp. VLSI Circuits (VLSIC)*, Jun. 2010, pp. 19–20.

[12] H. Kim, R. F. Yazicioglu, P. Merken, C. Van Hoof, and H.-J. Yoo, "ECG signal compression and classification algorithm with quad level vector for ECG holter system," *IEEE Trans. Inf. Technol. Biomed.*, vol. 14, no. 1, pp. 93–100, Jan. 2010.

[13] S.-Y. Lee, J.-H. Hong, C.-H. Hsieh, M.-C. Liang, S.-Y. C. Chien, and K.-H. Lin, "Low-power wireless ECG acquisition and classification system for body sensor networks," *IEEE J. Biomed. Health Informat.*, vol. 19, no. 1, pp. 236–246, Jan. 2015.

[14] Y.-P. Chen *et al.*, "An injectable 64 nW ECG mixed-signal SoC in 65 nm for arrhythmia monitoring," *IEEE J. Solid-State Circuits*, vol. 50, no. 1, pp. 375–390, Jan. 2015.

[15] J. Pan and W. J. Tompkins, "A real-time QRS detection algorithm," *IEEE Trans. Biomed. Eng.*, vol. BME-32, no. 3, pp. 230–236, Mar. 1985.

[16] A. H. Khandoker, M. H. Imam, J. P. Couderc, M. Palaniswami, and J. F. Jelinek, "QT variability index changes with severity of cardiovascular autonomic neuropathy," *IEEE Trans. Inf. Technol. Biomed.*, vol. 16, no. 5, pp. 900–906, Sep. 2012.

[17] N. Bayasi, T. Tekeste, H. Saleh, A. Khandoker, B. Mohammad, and M. Ismail, "Adaptive technique for P and T wave delineation in electrocardiogram signals," in *Proc. IEEE 36th Annu. Int. Conf. Eng. Med. Biol. Soc.*, Aug. 2014, pp. 90–93.

[18] P. Tadejko and W. Rakowski, "Mathematical morphology based ECG feature extraction for the purpose of heartbeat classification," in *Proc. IEEE 6th Int. Conf. Comput. Inf. Syst. Ind. Manage. Appl. (CISIM)*, Jun. 2007, pp. 322–327.

[19] K. Jen and Y. Hwang, "ECG feature extraction and classification using cepstrum and neural networks," *J. Med. Biol. Eng.*, vol. 28, no. 1, p. 31, 2008.

[20] Q. Zhao and L. Zhang, "ECG feature extraction and classification using wavelet transform and support vector machines," in *Proc. IEEE Int. Conf. Neural Netw. Brain (ICNN&B)*, vol. 2. Oct. 2005, pp. 1089–1092.

[21] T. Heeren and R. D'Agostino, "Robustness of the two independent samples t-test when applied to ordinal scaled data," *Statist. Med.*, vol. 6, no. 1, pp. 79–90, 1987.

[22] R. Kumar and A. Indrayan, "Receiver operating characteristic (ROC) curve for medical researchers," *Indian Pediatrics*, vol. 48, no. 4, pp. 277–287, 2011.

[23] A. L. Goldberger *et al.*, "Physiobank, physiotoolkit, and physionet: Components of a new research resource for complex physiologic signals," *Circulation*, vol. 101, no. 23, pp. e215–e220, Jun. 2000.

[24] J. J. Nobel. [Online]. Available: https://www.ecri.org/Products/Pages/AHA_ECG_DVD.aspx

Nourhan Bayasi (M'13) received the B.S. degree in electrical and computer engineering from the Khalifa University of Science, Technology and Research, Abu Dhabi, United Arab Emirates, in 2013, where she is currently pursuing the M.S. degree in electrical and computer engineering.

Her research project focuses on system-on-chip design and implementation of a fully integrated wearable biomedical system. Her current research interests include designing analog and mixed-signals integrated circuits, low power circuit design, and digital signal processing and its application.

Temesghen Tekeste (M'11) received the B.S. degree in electrical engineering from Asmara University, Asmara, Eritrea, in 2007, and the M.S. degree in microsystems engineering from the Masdar Institute of Science and Technology, Abu Dhabi, United Arab Emirates, in 2012. He is currently pursuing the Ph.D. degree with the Khalifa University of Science, Technology and Research, Abu Dhabi, with a focus on ultralow power digital circuit design.

He joined the Eritrea Institute of Technology, Abardae, Eritrea, as a Teaching Assistant and Laboratory Instructor in 2006. His current research interests include low-power, mixed-signal integrated circuit design that involved schematic design, simulation, layout, and verification of an ultralow power clock generator for heart rate sensor IC.

Hani Saleh (M'12–SM'14) received the B.S. degree in electrical engineering from the University of Jordan, Amman, Jordan, the M.Sc. degree in electrical engineering from the University of Texas at San Antonio, San Antonio, TX, USA, and the Ph.D. degree in computer engineering from the University of Texas at Austin, Austin, TX, USA.

He was with several leading semiconductor companies, including Intel, Santa Clara, CA, USA, where he was involved in ATOM mobile microprocessor design, AMD, Sunnyvale, CA, USA, where he was involved in Bobcat mobile microprocessor design, Qualcomm, San Diego, CA, USA, where he was involved in QDSP DSP core design for mobile systems-on-chip (SoCs), Synopsys, Mountain View, CA, USA, as a Key Member of the Synopsys Turnkey Design Group, where he taped out many application-specified integrated circuits (ASICs) and designed the I2C DW IP included in Synopsys DesignWare library, Fujitsu, Tokyo, Japan, where he was involved in SPARC compatible high performance microprocessor design, and Motorola Australia, Burwood East, VIC, Australia, where he was involved in M210 low power microprocessor synthesizable core design. He was a Senior Chip Designer (Technical Leader) with Apple Inc., Cupertino, CA, USA, where he was involved in the design and implementation of Apple next-generation graphics cores for its mobile products (iPad and iPhone). He has a total of 19 years of industrial experience in ASIC chip design, microprocessor design, DSP core design, graphics core design, and embedded system design. He is currently an Assistant Professor of Electronic Engineering with the Khalifa University of Science, Technology and Research, Abu Dhabi, United Arab Emirates. He is an Active Member with the Semiconductor Research Center, Khalifa University of Science, Technology and Research, where he leads a project for the development of wearable blood glucose monitoring SoC and a mobile surveillance SoC. His experience spans DSP core design, microprocessor peripherals design, microprocessors, and graphics core deign. He holds two issued U.S. patents, five pending patent applications, and has authored over 50 articles in peer-reviewed conferences and journals in digital system design, computer architecture, DSP, and computer arithmetic. His current research interests include DSP algorithms design, DSP hardware design, computer architecture, computer arithmetic, SoC design, ASIC chip design, FPGA design, and automatic computer recognition.

Baker Mohammad (M'04–SM'13) received the B.S. degree from the University of New Mexico, Albuquerque, NM, USA, the M.S. degree from Arizona State University, Tempe, AZ, USA, and the Ph.D. degree from the University of Texas at Austin, Austin, TX, USA, in 2008, all in electrical and computer engineering.

He was a Senior Staff Engineer and the Manager with Qualcomm, Austin, where he was involved in designing high performance and low power DSP processor used for communication and multimedia application. He was involved in a wide range of microprocessors design with Intel Corporation, Santa Clara, CA, USA, from high performance, server chips >100 W (IA-64), to mobile embedded processor low power sub-1 W (xscale). He has over 16 years of industrial experience in microprocessor design with an emphasis on memory, low power circuit, and physical design. He is currently an Assistant Professor of Electronic Engineering with the Khalifa University of Science, Technology and Research, Abu Dhabi, United Arab Emirates, and a Consultant with Qualcomm Inc., San Diego, CA, USA. In addition, he is involved in microwatt range computing platform for WSN focusing on energy harvesting and power management, including efficient dc/dc and ac/dc converters. He holds ten issued U.S. patents and has several pending patent applications. He has authored one book entitled *Embedded Memory Design for Multi-Core and SoC* and co-authored several publications in digital system design, memory design and testing, energy harvesting, power management, and power conversion, in addition to emerging memory technology modeling and design. His current research interests include power efficient computing, high yield embedded memory, and emerging technology, such as memristor, STTRAM, and computer architecture.

Dr. Mohammad has served the IEEE in many editorial and administrative capacities. He is a member of the Technical Program Committee of several IEEE conferences, such as the International Conference on Computer Design, the International Conference on Environmental and Computer Science, and the VLSI-SoC Conference. He is a Regular Reviewer of the IEEE TRANSACTIONS ON VLSI SYSTEMS and the IEEE TRANSACTIONS ON DESIGN AUTOMATION OF ELECTRONIC SYSTEMS. He is an Active Member of region eight student activities, including the Student Best Paper Competition, the UAE Chapter Student Day, and the KUSTAR Student Branch Advisor.

Ahsan Khandoker (M'07–SM'12) received the B.Sc. degree in electrical and electronic engineering from the Bangladesh University of Engineering and Technology, Dhaka, Bangladesh, in 1996, the M.Eng.Sc. degree from Multimedia University, Cyberjaya, Malaysia, in 1999, the M.Eng. degree in 2001, and the D.Eng. degree in physiological engineering from the Muroran Institute of Technology, Muroran, Japan, in 2004.

He has been with several Australian medical device manufacturing industries, and hospitals as a Research Consultant focusing on integration of technology in clinical settings. He is currently an Assistant Professor with the Department of Biomedical Engineering, Khalifa University of Science, Technology and Research, Abu Dhabi, United Arab Emirates. He is a Senior Research Fellow with the Australian Research Council Research Networks on Intelligent Sensors, Sensor Networks and Information Processing, University of Melbourne, Melbourne, VIC, Australia. He has authored 43 peer-reviewed journal articles and over 85 conference papers (an h-index of 16) in physiological signal processing and modeling in fetal cardiac disorders, sleep disordered breathing, diabetic autonomic neuropathy, and human gait dysfunction.

Mohammed Ismail (S'80–M'82–SM'84–F'97) spent over 25 years in academia and industry in the U.S. and Europe. He served as a Faculty Member with the Ohio State University's (OSU) ElectroScience Laboratory, Columbus, OH, USA. He was a Research Chair with the Swedish Royal Institute of Technology, Stockholm, Sweden, where he founded the Radio and Mixed Signal Integrated Systems Research Group. He held visiting appointments with Aalto University, Espoo, Finland, the Norwegian Institute of Technology, Trondheim, Norway, the University of Oslo, Oslo, Norway, Twente University, Enschede, The Netherlands, and the Tokyo Institute of Technology, Tokyo, Japan. He joined the Khalifa University of Science, Technology and Research, Abu Dhabi, United Arab Emirates, in 2011, where he holds the ATIC Professor Chair and is the Head of the Electrical and Computer Engineering Department, which exists on both campuses in Sharjah and Abu Dhabi. He advised the work of over 50 Ph.D. degree students and over 100 M.S. degree students. He has served as a Corporate Consultant to over 30 companies and is the Co-Founder of Micrys Inc., Columbus, Spirea AB, Stockholm, Firstpass Technologies Inc., Dublin, OH, USA, and ANACAD (currently part of Mentor Graphics), Cairo, Egypt. He is currently a prolific author and an entrepreneur in chip design and test. He is the Founder of the OSU's Analog VLSI Laboratory, one of the foremost research entities in the field of analog, mixed signal, and RF integrated circuits. He serves as the Director of KSRC and the Co-Director of the ATIC-SRC Center of Excellence on Energy Efficient Electronic Systems targeting self-powered chip sets for wireless sensing and monitoring, biochips, and power management solutions. He has authored or co-authored over 20 books and over 150 journal publications and holds eight U.S. patents issued and several pending. His current research interests include self-healing design techniques for CMOS RF and millimeter wave ICs in deep nanometer nodes.

Prof. Ismail received the U.S. Presidential Young Investigator Award, the Ohio State Lumley Research Award four times in 1992, 1997, 2002, and 2007, and the U.S. Semiconductor Research Corporations Inventor Recognition Award twice. He is the Founding Editor of the *Journal of Analog Integrated Circuits and Signal Processing* (Springer) and serves as the Journals Editor-in-Chief. He has served the IEEE in many editorial and administrative capacities. He is the Founder of the IEEE International Conference on Electronics, Circuits and Systems and the Flagship Region 8 Conference of the IEEE Circuits and Systems Society.